J. Phys. B: At. Mol. Opt. Phys. **31** (1998) L177–L185. Printed in the UK PII: S0953-4075(98)88276-X

LETTER TO THE EDITOR

Continuum states of HeH^+

Jonathan Tennyson†

Department of Physics and Astronomy, University College London, London WC1E 6BT, UK

Received 8 October 1997, in final form 5 January 1998

Abstract. *R*-matrix calculations are performed on $^1\Sigma^+$ symmetry resonance states of the HeH^+ for internuclear separations in the range 0.8–2.0 a_0. Position, widths and quantum defects are given for resonances converging on the $2s\sigma$, $2p\sigma$ and $2p\pi$ states of HeH^{2+}. Calculations focus on $^3HeT^+$ which is produced in β decay of T_2 and is thus important for neutrino mass measurements. The resonances may also be important in He^{2+}–H^- collisions.

Whether or not neutrinos are massless remains one of the key unresolved questions of modern science. A number of methods have been tried to determine the mass of the neutrino. The best laboratory determinations of the electron–neutrino mass come from measuring the energy spectrum of the β electrons in the decay (Holzschuh 1992)

$$T_2 \rightarrow {}^3HeT^+ + \bar{\nu}_e + e^-. \tag{1}$$

So far the most reliable determinations yield a value for the square of the neutrino mass which is negative! These determinations depend not only on accurate measurements but also on a knowledge of how energy is distributed in the molecular product $^3HeT^+$. This information comes largely from quantum mechanical calculations (e.g. Jeziorski *et al* 1985a, b, Froelich *et al* 1987, 1993, Froelich and Saenz 1996). Despite detailed analysis (Saenz and Froelich 1997a, b), this discrepancy remains.

A number of possible sources of discrepancy remain to be explored, some of them experimental. One possible problem is that, thus far, theoretical treatments of the continuum states of $^3HeT^+$ (Martin and Cohen 1985, Froelich *et al* 1987, Szalewicz *et al* 1987, Froelich *et al* 1993) have been limited both in terms of the resonances states of $^3HeT^+$ considered and their variation as a function of internuclear separation, although recently Saenz and Froelich (1997b) have explicitly considered the effects of nuclear motion for a few low-lying resonances.

In this work I report a systematic, geometry-dependent, treatment of the resonant states of $^3HeT^+$. It should be noted that resonant states of the HeH^+ system also arise in He^{2+}–H^- collisions (Terao *et al* 1988, Cherkani *et al* 1991a, b).

Calculations

Calculations were performed using the UK molecular *R*-matrix programs (Gillan *et al* 1995), using an *R*-matrix sphere of 10 a_0. Electron collisions from a 'HeH^{2+}' target were considered for He–H separations of $R = 0.8$, 1.0, 1.2, 1.3, 1.4, 1.5, 1.6, 1.8 and 2.0 a_0. The

† E-mail address: j.tennyson@ucl.ac.uk

0953-4075/98/040177+09$19.50

$1s\sigma, 2s\sigma, 2p\sigma$ and $2p\pi$ states of HeH^{2+} were included in the close-coupling expansion. These states were represented by (3s, 2p, 1d) Slater-type orbitals on each atom. Exponents were optimized for all four states at $R = 1.4\ a_0$ by comparison with exact numerical energies computed using the code due to Power (1973). Energies of the target states used in this calculation are given in table 1.

Table 1. Computed HeH^{2+} 'target' energy levels, in E_h, as a function of internuclear separation, R in a_0.

R	$1s\sigma$	$2s\sigma$	$2p\pi$	$2p\sigma$
0.8	−0.736 93	1.221 59	1.444 83	1.567 45
1.0	−1.031 36	0.670 17	0.971 75	1.116 02
1.2	−1.204 15	0.301 99	0.666 63	0.829 12
1.3	−1.265 78	0.163 76	0.552 77	0.723 06
1.4	−1.316 84	0.048 63	0.457 28	0.634 49
1.5	−1.360 05	−0.047 45	0.376 42	0.559 74
1.6	−1.397 31	−0.127 74	0.307 40	0.496 06
1.8	−1.458 83	−0.251 13	0.196 73	0.394 08
2.0	−1.507 88	−0.337 81	0.113 12	0.316 12

The continuum was represented by 65σ and 54π functions obtained by solving for a Coulomb potential ($(V = -2/r)$ in au) inside the R-matrix sphere using a partial-wave expansion with $l \leqslant 6$. To mitigate linear dependence effects, two σ and one π continuum functions were removed from the basis using Lagrange orthogonalization (Tennyson *et al* 1987). The remaining continuum orbitals were Schmidt orthogonalized to the entire set of target functions.

Inside the R-matrix sphere the wavefunction of HeH^+ is written as

$$\Psi = \mathcal{A} \sum_{i=1}^{4} \sum_{j} a_{ij} \Phi_i F_{ij} + \sum_{j} b_j X_j \tag{2}$$

where Φ_i are the HeH^{2+} 'target' states and F_{ij} are the continuum orbitals. The X_j are L^2 configurations which are included to relax the orthogonalization conditions discussed above and to allow for polarization effects additional to those given by the close-coupling expansion, see Gillan *et al* (1995) for a full discussion. As the HeH^{2+} target only has one electron, all symmetry-allowed configurations with two electrons in any target orbital were included as there is no danger of over-correlation for this system.

In the outer region R-matrices were propagated to 50 a_0 (Morgan 1984) and then K-matrices obtained using a Gailitis expansion (Noble and Nesbet 1984). All calculations were performed for $^1\Sigma^+$ total symmetry as this is the relevant one for T_2 β-decay (Fackler *et al* 1985).

Resonances were detected using an energy grid of $0.000\,25 E_h$ and then fitted automatically assuming a Breit–Wigner form for an isolated resonance (Tennyson and Noble 1984). Fits were performed for 20 points in a region given approximately by $E_{\rm res} \pm \Gamma$. Fits assumed an eigenphase sum, η, whose background varied linearly in this region. In some cases it was necessary to rerun the resonance fit to improve the fit. As shown below, this method missed some narrow resonances ($\Gamma < 10^{-4} E_h$), these are unlikely to play a major role in the T_2 β-decay experiment. There are a considerable number of crossings between resonances and of resonances crossing thresholds belonging to lower target states, see figure 1. Resonance fits were generally poorer in these crossing regions. For this reason

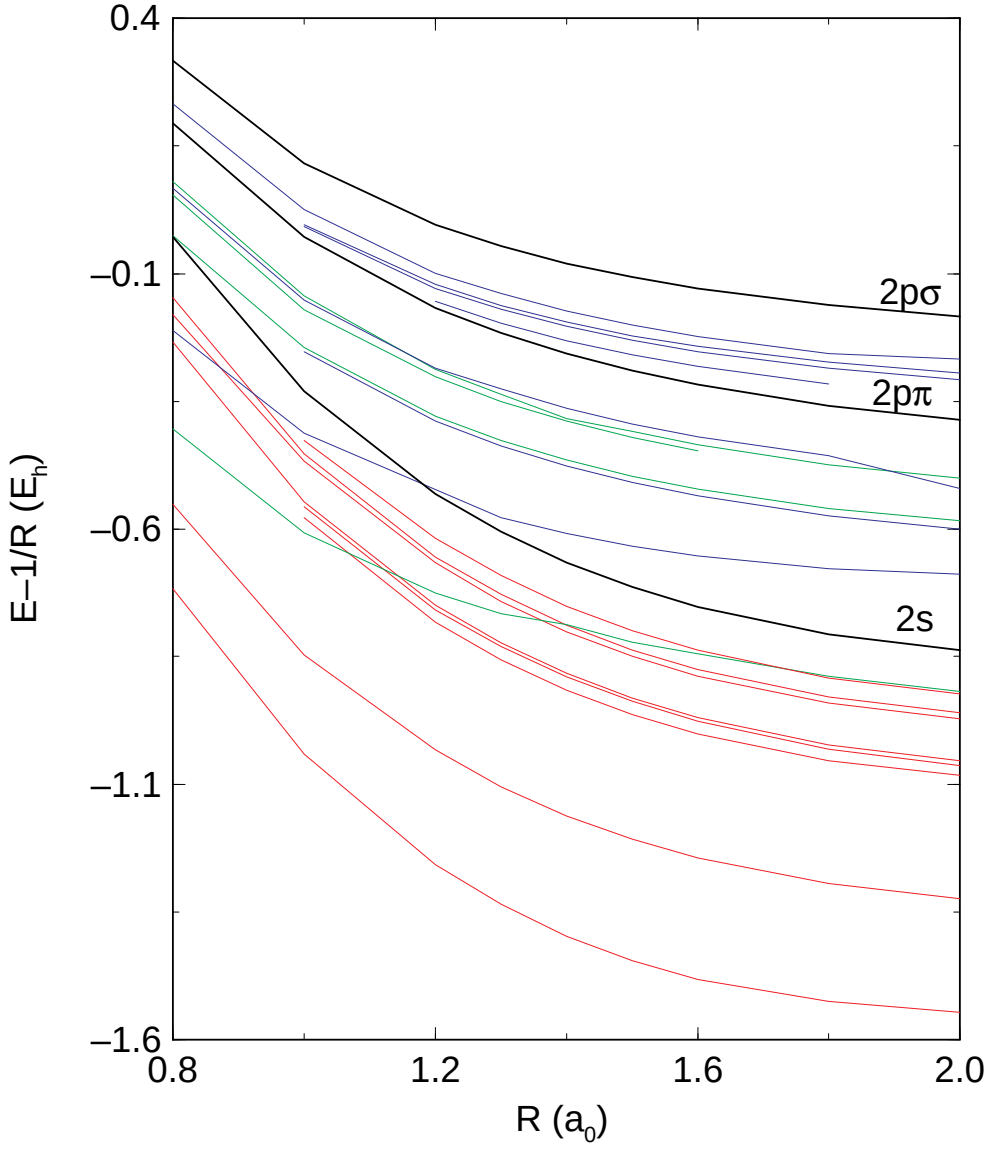

Figure 1. HeH^+ resonance curves and HeH^{2+} target potential (labelled) as a function of internuclear separation. The R^{-1} term removes the effects of the H^+–He^+ Coulomb repulsion. Resonances converging to the 2s, 2pπ and 2pσ target states are drawn in red, green and blue, respectively.

Table 2. Position, E_{res}, and width, Γ, of the low-lying resonances in the HeH^+ system at $R = 1.4\ a_0$.

	Froelich *et al* (1993)		This work	
	E_{res} (E_h)	Γ (E_h)	E_{res} (E_h)	Γ (E_h)
2s2pσ	−0.688 14	0.024 29	−0.683 47	0.024 93
2s3s	−0.451 15	0.018 76	−0.447 62	0.017 12
2s3pσ	−0.209 93	0.005 09	−0.201 65	0.003 45
2s3dσ	−0.185 14	0.003 75	−0.175 50	0.001 87
2s4s	−0.177 11	0.002 94	−0.168 89	0.003 60
2s4pσ			−0.087 57	0.000 98
2s4fσ			−0.076 52	0.000 07
2s5s			−0.074 26	0.001 40
2pπ^2			−0.073 52	0.001 92
2s5pσ			−0.036 97	0.000 69
2pσ^2			−0.031 34	0.003 24
2s6s			−0.030 35	0.000 79
2s6pσ			−0.010 14	0.000 36

a goodness factor, gf, was defined which enables the quality of the fit to be assessed by analysing the sum of the residues:

$$gf = -\log_{10}\left|\sum_{i=1}^{20}\eta_{fit}(E_i) - \eta_{calc}(E_i)\right|. \tag{3}$$

Satisfactory fits should have $gf \geqslant 4$. Experience has shown that fits with $gf = 2$ give reliable positions, E_{res}, but widths, Γ, which are often too large. Results with $gf \leqslant 0$ are unreliable.

Results

Table 2 compares results of the present calculations with those of Froelich *et al* (1993). These workers used highly accurate electronic wavefunctions specifically designed to treat two-electron systems. One would therefore expect their resonance positions, at least for the lowest resonances, to be variationally better, i.e. lower, than those computed here. Conversely Froelich *et al* used a complex coordinate method (Froelich *et al* 1987) which, given their approximate representation of the continuum, is unlikely to yield resonance widths as accurately as the method used here. Froelich *et al* number but do not assign their resonances, so the assignments come from the quantum defect analysis discussed below. The resonances from the two calculations have been matched on energy ordering. This is clearly satisfactory for the lowest three resonances, but it is possible that the higher two resonances should be swapped. The agreement between the two calculations for the lower three resonances is very satisfactory.

The resonance positions and widths from the present calculations are subjected to two types of error. Firstly, they are not calculated directed but only by fitting; the error in these fits is quantified by gf. Secondly, there are errors in the model which are largely due to truncation of the basis set and coupled-states expansion. It is difficult to precisely quantify this second error, but experience shows that improvements lead to the resonances appearing at lower energies and becoming narrower.

Figure 1 gives the resonance curves for the major resonances treated in this work. Also shown are the $n = 2$ states of HeH^{2+} to which these resonances converge. The

resonance and target state energies in the figure have had R^{-1} subtracted from them. This term corresponds to the Coulomb repulsion between He^+ and H^+ fragments into which the HeH^{2+} states dissociate. Removal of the R^{-1} term makes the curves less steep and highlights the various crossings. Even with the underlying Coulomb repulsion removed, both resonance and target state curves still appear to be repulsive. This is not true of the HeH^{2+} ground state (not plotted) which has a shallow minimum, at about $R = 1.3\ a_0$ in this representation.

At a given internuclear separation, each electronic state of a diatomic molecular ion supports a Rydberg series of electronic states with one member for each (n, ℓ) combination with $n > \ell$. Thus means that below each HeH^{2+} curve depicted in figure 1 there should be an infinite number of increasingly narrow resonances. Not only are the higher resonances omitted from this figure, and the results tabulated below, but some of the low-lying narrow (d- and f-wave) resonances have also been ignored.

Table 3 presents position widths and effective quantum numbers, ν (Seaton 1983), for the 19 dominant (i.e. broadest) resonances in the energy region up to about 100 eV above the $^3HeT^+$ ($R = 1.4$) ground state energy. This is an energy region in which fits to the experimental T_2 decay data do not match the theoretical distributions particularly well (Jonsell and Monkhorst 1996, Saenz and Froelich 1997b).

The effective quantum numbers for each series in table 3 are given relative to the ion curve associated with the assignment. The smooth and gentle variation of the quantum defects with bond length makes this association clear cut. Each state is also assigned an $n\ell$ quantum number for the second 'Rydberg' electron. These assignments were chosen using the values of the quantum defects, but should not be regarded as definitive; particularly for the higher-lying resonances where the absence of some series makes these assignments somewhat arbitrary.

The situation with assignments is also clouded by the many crossings. This appears to be particularly so for resonances associated with the $2p\sigma$ target state where there is considerable s–d mixing. Indeed the $2p\sigma$–$3p\sigma$ resonance width appears to go to zero at $R = 1.2\ a_0$, giving a so-called 'bound state in the continuum' for that geometry. This behaviour is known to be a feature of certain resonance crossings (Collins *et al* 1986).

Discussion and conclusions

Modelling the neutrino mass experiments is a complicated problem with many aspects that need to be addressed (Saenz and Froelich 1997a, b). Thus theoretical studies, focusing on bound states of $^3HeT^+$, have suggested that the effects of including nuclear motion in the models is small (Jeziorski *et al* 1985b). However, the behaviour of the resonance potentials, as illustrated in figure 1, is somewhat different from that of, at least, the lower-lying bound states of $^3HeT^+$. As the resonances track strongly repulsive states of HeH^{2+}, they show a very strong dependence on internuclear separation. This will mean that, when nuclear motion effects are considered, each resonance will have an influence over a wider range of energies than is suggested by their generally rather narrow width. This broadening of the resonances was found in the recent study of Saenz and Froelich (1997b).

A further complication is that, of course, there are infinite series of resonances converging to each electronically excited state of HeH^{2+}. Quite what effect these infinite series of increasingly narrow resonances has remains an open question. However, it should be pointed out that no model of the T_2 β-delay has yet included the infinite series of electronically bound Rydberg states which converge to the HeH^{2+} ground state. It would seem likely that the effect due to these lower-lying states will be more important.

Table 3. Resonance position, $E_{\rm res}$, and width, Γ, for $^1\Sigma$ symmetry states of HeH^+, both in E_h as a function of internuclear separation, R in a_0. Also given are assignments, effective quantum numbers (ν), relative to the appropriate threshold and the goodness factor, gf, of the fit (see text for further details).

R	$E_{\rm res}$	Γ	ν	gf
2s2pσ				
0.8	0.532 50	0.022 61	1.704	7
1.0	−0.041 10	0.026 42	1.677	7
1.2	−0.424 14	0.023 16	1.660	5
1.3	−0.566 48	0.026 30	1.655	7
1.4	−0.683 47	0.024 94	1.653	7
1.5	−0.779 36	0.023 03	1.653	8
1.6	−0.857 65	0.020 77	1.655	8
1.8	−0.970 21	0.015 90	1.665	8
2.0	−1.046 95	0.011 46	1.679	9
2s3s				
0.8	0.697 96	0.016 48	1.954	8
1.0	0.153 16	0.017 15	1.967	8
1.2	−0.199 87	0.019 72	1.996	5
1.3	−0.336 14	0.017 73	2.000	8
1.4	−0.447 63	0.017 12	2.008	9
1.5	−0.540 92	0.016 31	2.013	9
1.6	−0.619 07	0.015 33	2.018	9
1.8	−0.739 48	0.013 20	2.024	9
2.0	−0.824 03	0.011 29	2.028	9
2s3pσ				
0.8				
1.0	0.421 74	0.003 74	2.837	6
1.2	0.050 00	0.001 20	2.817	6
1.3	−0.086 82	0.003 86	2.825	6
1.4	−0.201 63	0.003 40	2.827	6
1.5	−0.297 21	0.002 01	2.830	6
1.6	−0.376 77	0.002 56	2.834	6
1.8	−0.498 22	0.001 74	2.845	6
2.0	−0.582 86	0.001 08	2.857	5
2s3dσ				
0.8				
1.0	0.443 27	0.002 24	2.969	6
1.2	0.074 36	0.004 38	2.964	4
1.3	−0.061 33	0.002 60	2.981	4
1.4	−0.175 48	0.001 99	2.987	3
1.5	−0.271 28	0.001 65	2.989	3
1.6	−0.351 67	0.001 45	2.989	3
1.8	−0.476 01	0.001 52	2.982	4
2.0	−0.564 07	0.001 76	2.973	4
2s4s				
0.8	1.016 08	0.001 96	3.120	5
1.0	0.453 34	0.001 63	3.038	5
1.2	0.083 56	0.001 18	3.026	4
1.3	−0.053 69	0.003 06	3.033	4
1.4	−0.168 85	0.003 50	3.033	3
1.5	−0.264 85	0.003 94	3.033	3
1.6	−0.344 92	0.003 96	3.035	3
1.8	−0.467 89	0.003 63	3.038	4
2.0	−0.554 23	0.003 10	3.040	4

Table 3. Continued.

R	E_{res}	Γ	ν	gf
2s4pσ				
0.8	1.070 21	0.001 88	3.635	6
1.0	0.533 18	0.001 50	3.821	5
1.2	0.167 16	0.002 07	3.851	4
1.3	0.027 35	0.001 43	3.829	6
1.4	−0.087 52	0.001 09	3.833	4
1.5	−0.183 30	0.001 10	3.837	4
1.6	−0.263 20	0.000 94	3.842	3
1.8	−0.385 73	0.000 62	3.855	4
2.0	−0.471 81	0.000 37	3.863	8
2s5s				
0.8	1.103 11	0.000 54	4.107	6
1.0	0.546 74	0.000 81	4.025	5
1.2	0.177 83	0.000 24	4.014	0
1.3	0.040 78	0.001 38	4.033	6
1.4	−0.074 26	0.001 40	4.034	2
1.5	−0.170 44	0.001 59	4.033	3
1.6	−0.250 66	0.001 55	4.034	3
1.8	−0.373 84	0.001 58	4.037	3
2.0	−0.460 29	0.001 30	4.041	5
2pπ^2				
0.8	0.846 38	0.008 01	1.828	8
1.0	0.391 96	0.008 12	1.857	5
1.2	0.107 22	0.008 69	1.891	6
1.3	0.003 74	0.006 13	1.909	6
1.4	−0.073 52	0.001 92	1.941	2
1.5	−0.154 86	0.004 53	1.940	5
1.6	−0.219 16	0.004 80	1.949	5
1.8	−0.332 88	0.001 02	1.946	4
2.0	−0.418 28	0.000 68	1.938	3
2s5pσ				
0.8				
1.0	0.573 66	0.000 38	4.552	5
1.2	0.214 57	0.001 53	4.783	5
1.3	0.077 98	0.000 71	4.829	5
1.4	−0.036 97	0.000 69	4.834	4
1.5	−0.132 84	0.000 65	4.840	4
1.6	−0.212 77	0.000 88	4.850	5
1.8	−0.336 25	0.000 25	4.847	6
2.0	−0.422 64	0.000 18	4.856	3
2pσ^2				
0.8	1.038 95	0.003 45	1.945	6
1.0	0.587 19	0.002 66	1.945	0
1.2				
1.3	0.190 91	0.009 60	1.938	8
1.4	0.105 03	0.008 92	1.944	8
1.5	0.032 96	0.008 34	1.948	8
1.6	−0.027 71	0.007 86	1.954	8
1.8	−0.122 29	0.007 23	1.966	8
2.0	−0.189 15	0.007 12	1.990	8

Table 3. Continued.

R	E_{res}	Γ	ν	gf
2pσ 4s				
0.8				
1.0	0.747 04	0.004 81	2.983	2
1.2	0.444 30	0.004 44	2.999	4
1.3	0.331 70	0.003 95	3.008	4
1.4	0.237 38	0.003 82	3.016	8
1.5	0.157 60	0.003 67	3.023	4
1.6	0.089 67	0.003 52	3.031	5
1.8	−0.018 84	0.003 31	3.046	5
2.0	−0.100 36	0.003 18	3.061	5
2pπ 3dπ				
0.8	1.224 59	0.005 87	3.013	2
1.0	0.754 93	0.003 56	3.037	3
1.2	0.454 76	0.002 45	3.072	4
1.3	0.342 31	0.002 54	3.083	4
1.4	0.248 82	0.002 55	3.097	4
1.5	0.169 87	0.002 36	3.112	5
1.6	0.102 75	0.002 33	3.126	4
1.8	−0.004 20	0.002 34	3.155	4
2.0	−0.084 15	0.002 33	3.184	6
2pπ 4pπ				
0.8	1.304 23	0.010 13	3.772	3
1.0	0.829 38	0.006 22	3.748	4
1.2	0.531 63	0.006 54	3.849	3
1.3	0.418 84	0.004 87	3.864	4
1.4	0.325 36	0.004 33	3.891	6
1.5	0.245 99	0.004 11	3.916	3
1.6	0.178 43	0.004 20	3.938	2
1.8				
2.0				
2pπ 4dπ				
0.8	1.330 94	0.003 29	4.191	4
1.0	0.856 53	0.000 56	4.166	5
1.2	0.546 06	0.001 33	4.027	7
1.3	0.432 89	0.001 20	4.084	7
1.4	0.330 53	0.001 16	4.099	6
1.5	0.258 33	0.001 05	4.115	6
1.6	0.190 15	0.001 03	4.130	6
1.8	0.081 10	0.001 04	4.159	5
2.0	−0.000 93	0.001 07	4.188	5
2pσ 3pσ				
0.8	1.317 80	0.001 63	2.830	2
1.0	0.848 51	0.001 89	2.734	4
1.2	0.548 35	0.000 00	2.669	7
1.3	0.443 75	0.001 99	2.676	7
1.4	0.350 56	0.002 61	2.654	5
1.5	0.271 98	0.003 19	2.636	5
1.6	0.205 19	0.003 81	2.622	5
1.8	0.099 04	0.005 12	2.604	6
2.0	−0.020 37	0.006 67	2.600	4

Table 3. Continued.

R	E_{res}	Γ	ν	gf
2pσ 4pσ				
0.8				
1.0				
1.2	0.678 68	0.007 33	3.646	4
1.3	0.572 62	0.006 82	3.646	4
1.4	0.483 18	0.006 31	3.636	4
1.5	0.407 52	0.006 29	3.625	4
1.6	0.343 04	0.006 07	3.615	4
1.8	0.239 77	0.005 79	3.600	5
2.0	0.161 46	0.005 72	3.339	5
2pσ5s				
0.8				
1.0	0.992 61	0.003 54	4.026	3
1.2	0.704 42	0.004 30	4.005	4
1.3	0.599 42	0.002 48	4.022	3
1.4	0.510 93	0.002 28	4.022	3
1.5	0.436 15	0.002 24	4.023	3
1.6	0.372 54	0.001 99	4.024	3
1.8	0.270 68	0.001 59	4.026	3
2.0	0.192 76	0.001 21	4.027	4
2pσ 4dσ				
0.8				
1.0	0.996 30	0.001 51	4.087	3
1.2	0.712 16	0.001 13	4.135	3
1.3	0.606 63	0.001 08	4.145	4
1.4	0.519 06	0.000 96	4.164	4
1.5	0.445 19	0.000 96	4.178	4
1.6	0.382 38	0.000 94	4.194	5
1.8	0.282 00	0.000 95	4.224	5
2.0	0.205 37	0.001 06	4.250	7
2pσ 5pσ				
0.8	1.482 42	0.003 39	4.830	3
1.0	1.025 02	0.003 58	4.688	3
1.2	0.734 22	0.003 38	4.591	4
1.3	0.630 42	0.003 02	4.646	4
1.4	0.541 45	0.002 86	4.636	4
1.5	0.466 26	0.002 75	4.626	4
1.6	0.402 21	0.002 65	4.616	4
1.8	0.299 59	0.002 53	4.601	4
2.0	0.232 38	0.002 52	4.595	4

In summary, R-matrix calculations have been performed which give positions and widths of the broadest resonant states of the HeH^+ system as a function of internuclear separation. These resonances could be important for modelling both the β-decay of T_2, used in attempts to measure the mass of the neutrino. These autoionizing resonances also play a role in H^-–He^{2+} collisions and isoelectronic collision systems such as H^+–He or H–He^+.

I would like to thank Krzysztof Szalewicz for drawing this problem to my attention to the neutrino mass problem, Mariko Terao-Dunseath for alerting me to the He^{2+}–H^- problem and Alejandro Saenz for stimulating my interest with his excellent thesis. Much of this work was performed while I was on sabbatical at the Institute for Theoretical Atomic

and Molecular Physics at Harvard–Smithsonian Center for Astrophysics and JILA at the University of Colorado. I thank them for their hospitality and EPSRC for support through various grants.

References

Cherkani M H, Szucs S, Hus H and Brouillard F 1991a *J. Phys. B: At. Mol. Opt. Phys.* **24** 2367–77
Cherkani M H, Szucs S, Terao M, Hus H and Brouillard F 1991b *J. Phys. B: At. Mol. Opt. Phys.* **24** 209–18
Collins L A, Schneider B I, Noble C J, McCurdy C W and Yabushita S 1986 *Phys. Rev. Lett.* **57** 980–3
Fackler O, Jeziorski B, Kolos W, Monkhorst J H and Szalewicz K 1985 *Phys. Rev. Lett.* **55** 1388–91
Froelich P, Jeziorski B, Kolos W, Monkhorst H, Saenz A and Szalewicz K 1993 *Phys. Rev. Lett.* **71** 2871–4
Froelich P and Saenz A 1996 *Phys. Rev. Lett.* **77** 4724–7
Froelich P, Szalewicz K, Jeziorski B, Kolos W and Monkhorst H J 1987 *J. Phys. B: At. Mol. Phys.* **20** 6173–87
Gillan C J, Tennyson J and Burke P G 1995 *Computational Methods for Electron–Molecule Collisions* ed W M Huo and F A Gianturco (New York: Plenum)
Holzschuh E 1992 *Rep. Prog. Phys.* **55** 1035–91
Jeziorski B, Kolos W, Szalewicz K, Fackler O and Monkhorst J H 1985a *Phys. Rev.* A **31** 551–5
——1985b *Phys. Rev.* A **32** 2573–83
Jonsell S and Monkhorst J H 1996 *Phys. Rev. Lett.* **76** 4476–9
Martin R L and Cohen J S 1985 *Phys. Lett.* **110A** 95–8
Morgan L A 1984 *Comput. Phys. Commun.* **31** 419–22
Noble C J and Nesbet R K 1984 *Comput. Phys. Commun.* **33** 399–411
Power J D 1973 *Quantum Chem. Program Exchange* **11** 233
Saenz A and Froelich P 1997a *Phys. Rev.* C **56** 2132–61
——1997b *Phys. Rev.* C **56** 2162–84
Seaton M J 1983 *Rep. Prog. Phys.* **46** 167–257
Szalewicz K, Fackler O, Jeziorski B, Kolos W and Monkhorst J H 1987 *Phys. Rev.* A **35** 965–79
Tennyson J, Burke P G and Berrington K A 1987 *Comput. Phys. Commun.* **47** 207–12
Tennyson J and Noble C J 1984 *Comput. Phys. Commun.* **33** 421–4
Terao M, Harel C, Salin A and Allan R J 1988 *Z. Phys.* D **7** 319–32